Published in final edited form as:
Ann Biomed Eng. 2010 March ; 38(3): 558–569. doi:10.1007/s10439-009-9858-z.

Lipids and collagen matrix restrict the hydraulic permeability within the porous compartment of adult cortical bone

Demin Wen[1,2,*], **Caroline Androjna**[1,*], **Amit Vasanji**[1], **Joanne Belovich**[2], and **Ronald J. Midura**[1,#]

[1]Department of Biomedical Engineering, Lerner Research Institute, Cleveland Clinic, Cleveland, Ohio 44195 USA

[2]Department of Chemical and Biomedical Engineering, Cleveland State University, Cleveland, Ohio 44115 USA

Abstract

In vivo the hydraulic permeability of cortical bone influences the transport of nutrients, waste products and signaling molecules, thus influencing the metabolic functions of osteocytes and osteoblasts. In the current study two hypotheses were tested: the presence of (1) lipids and (2) collagen matrix in the porous compartment of cortical bone restricts its permeability. Our approach was to measure the radial permeability of adult canine cortical bone before and after extracting lipids with acetone-methanol, and before and after digesting collagen with bacterial collagenase. Our results showed that the permeability of adult canine cortical bone was below 4.0×10^{-17} m^2, a value consistent with prior knowledge. After extracting lipids, permeability increased to a median value of 8.6×10^{-16} m^2. After further digesting with collagenase, permeability increased to a median value of 1.4×10^{-14} m^2. We conclude that the presence of both lipids and collagen matrix within the porous compartment of cortical bone restricts its radial permeability. These novel findings suggest that the chemical composition of the tissue matrix within the porous compartment of cortical bone influences the transport and exchange of nutrients and waste products, and possibly influences the metabolic functions of osteocytes and osteoblasts.

Keywords

Cortical bone; Lipids; Collagen; Hydraulic permeability; Porosity

Introduction

Adult cortical bone tissue is a biocomposite material which is composed of 67% mineral salts and 33% organic matrix containing 62% type I collagen, 26% minor collagens and non-collagenous proteins, 6% lipids and 6% complex carbohydrates by dry weight.[9, 19] It is separated into two generalized compartments based on fluid accessibility: a non-porous compartment and a porous compartment comprising 90~95% and 5~10% of its volume, respectively.[17, 18, 31] This porous compartment contains vascular channels (Haversian and Volkmann's canals) interconnected by a lacuna-canalicular system filled with osteocytes, their filipodial extensions and a surrounding pericellular matrix.[4, 7, 28, 31] Biological fluids flow

#Corresponding author: Ronald J. Midura, Ph.D., Dept. of Biomedical Engineering, ND20, Lerner Research Institute, Cleveland Clinic, Cleveland, Ohio 44195 USA; 216/445-3212 (office); 216/444-9198 (fax); midurar@ccf.org.
*Equal contributions as first authors

within this porous compartment of cortical bone thereby providing a system to exchange nutrients and metabolic waste products.

Fluids are thought to flow through cortical bone as a result of mechanical deformation of bone tissue and/or by pressure gradients generated by vascular tissues inside cortical bone.[3, 5, 10, 12, 29] Fluid-flow in the lacuna-canalicular system of cortical bone is considered important to maintain osteocyte viability. Moreover the shear stresses generated from this fluid flow activate osteocytes which transduce this physical stimulus into biochemical signals that regulate extracellular matrix secretion in bone tissue.[6, 13, 14] Radial movements of water, nutrients and waste products in cortical bone is considered important given that the majority of vascular beds are located within the medullary cavity of bone adjacent to the endosteum, within the apical, non-osseous layers of the periosteum, and within Haversian and Volkmann's canals. Ultimately, fluids must flow from these vascular sources to adjacent areas of cortical bone in a radial direction, thus providing a rationale for studying the radial hydraulic permeability of cortical bone.

Hydraulic permeability is defined as the ease with which a fluid passes through a porous material and can be determined from Darcy's Law.[21, 22] To date, only a few studies have experimentally measured the hydraulic permeability of cortical bone in part because of the engineering challenges in measuring very low permeabilities. Such devices require high pressure tolerances in both the bone tissue holding chamber and other upstream components in order to accurately measure the permeability of cortical bone. Johnson et al.[12] determined that the radial permeability of bone containing large pores was 2.5×10^{-14} m^2. Li et al.[16] measured the permeability of adult canine versus puppy cortical bone devoid of large pores. They reported the radial permeability of adult canine tibial cortex was 5×10^{-17} m^2 and that the radial permeability of puppy bone was 6-fold higher than that of adult canines. In addition, they reported that the periosteal portion of cortical bone was relatively impermeable as compared to the endosteal portion of cortical bone since 0.5–1.0 mm of bone needed to be removed from the periosteal surface in order to make accurate measurements. Beno et al.[1] calculated the permeability within cortical bone based on finite elemental analysis using microstructural measurements of the lacuna-canalicular system. They predicted that the permeability of cortical bone strictly at the lacuna-canalicular level was in the range of $10^{-18} \sim 10^{-20}$ m^2.

Fluid flow through tissue matrices is influenced by a tissue's chemical composition (i.e., hydrophilicity versus hydrophobicity) and the orientation, packing density and extent of cross-linking of its matrix molecules.[26] Densely packed collagen fibers have been identified in the pericellular matrix of Haversian and Volkmann's canals[4, 7] and within osteocyte lacunae[7, 28]. Various lipids have been detected in both the porous and non-porous compartments of cortical bone.[9, 11, 15, 19, 30] While prior studies have provided accurate assessments of the radial permeability of adult cortical bone, there have not been any prior reports addressing what contributions its chemical compositions have on the hydraulic permeability within the porous compartment of cortical bone. For example, prostaglandins, steroids such as estrogen, and 1,25-dihydroxy-vitamin D3 are potent osteogenic agents that are derived from lipid substrates. Their amphipathic chemistry and small size should permit them to freely distribute both within the hydrophilic fluid phase of bone and distribute within hydrophobic phases in bone. Thus, a better understanding of the factors that regulate fluid flow inside bone tissue may in turn provide a better assessment of osteocyte physiology and inform *in vitro* bone tissue engineering approaches on the design of new bone scaffolds that better mimic *in vivo* fluid flow properties.[10, 21]

Accordingly, the current study investigated the influence of resident lipids and pericellular collagen matrix on the radial hydraulic permeability of the porous compartments in cortical

bone. To these ends, we designed a device to assess radial hydraulic permeability of cortical bone enabling repeated measures on the same bone wafers before and after sequential chemical or enzymatic treatments. We hypothesized that (1) the presence of hydrophobic molecules within the porous compartment of cortical bone would reduce its permeability, and that removal of such hydrophobic materials would increase its permeability; and (2) the presence of a collagen-containing pericellular matrix within the porous compartment of cortical bone would reduce its permeability, and that digestion of this collagenous matrix would increase its overall permeability.

Material and Methods

All bone tissues were obtained from animals that had been sacrificed in the course of IACUC approved research investigations conducted elsewhere at this institution. Mid-diaphyseal portions of tibia were harvested from outbred adult canines (~25–30 kg body weight). Periosteal tissue layers, including most of the basal cambium cell layer, were stripped off the bone by dissection. Bone marrow was flushed out of the bone with phosphate buffer saline (PBS) (Cellgro). These tibial diaphyses were then stored in PBS with 0.05% sodium azide (Sigma) at 4° C and used within a 2-week period from collection (referred to as “unprocessed”). To assure that changes did not occur during storage, some bone samples were used immediately as fresh samples for hydraulic permeability assessments.

Thin sections were cut from tibial diaphyses in a cross-sectional plane and stained with basic fuchsin to reveal Haversian and Volkmann’s canals. Such histological analysis indicated that the presence and orientation of Haversian and Volkmann’s canals were different in the periosteal versus the endosteal halves of canine cortical bone (Fig. 1A). In the endosteal half more of the Volkmann’s canals appeared to traverse radially throughout this half of the cortex. Thus, in agreement with assessments by Li et al.[16], the endosteal halves were considered to be more appropriate for radial hydraulic permeability measurements than their corresponding periosteal halves.

Based on the above histological findings, this study focused on measuring radial hydraulic permeability of bone wafers from the endosteal halves of these adult canine tibial diaphyses. Bone wafers with approximate dimensions of 15 mm length, 15 mm width, and 1.5 mm thick were cut from the diaphyseal portions of tibial cortices with an EXTEC ® Labcut 1010 Low Speed Diamond Saw (EXTEC Corp). Endosteal bone wafers from the medial and lateral aspects of the diaphyseal cortex (over the entire superior to inferior axis, see shaded regions in Fig. 1B) were separately collected and stored in PBS with 0.05% sodium azide in pre-weighed glass bottles. A total of 27 bone wafers were collected from 2 different dogs: 13 from one and 14 from the other.

Porosity of fresh bone wafers was measured as follows. Micro-computed tomography (micro-CT) volumes of bone samples were acquired using a SkyScan 1172 (3 μm voxel resolution) *ex vivo* imaging system. Porosity analysis was performed using Matlab R2008a (MathWorks), Image Pro-Plus v6.1 (Media Cybernetics), VolSuite (Ohio Supercomputer Center, Columbus, OH), and MicroView v2.2 (GE Healthcare). Briefly, volumes (~1800 × 1000 × 1000 voxels) were rotated and cropped using VolSuite, and imported into Image-Pro as individual image stacks. In each plane of a particular stack, a median filter was applied to remove noise, holes were filled using a morphological "closing" filter, and bone outgrowths from the endosteal surface were removed using a watershed filter. The resulting contiguous, "filled" bone volumes were then multiplied by an inverted and thresholded version of their corresponding original volume to reveal porous content that was further filtered in Matlab to remove pores below a given volumetric threshold (connected components algorithm). Subsequently, total pore volume was calculated and porous volumes in both the axial and radial directions were

generated (a pore was defined as radially localized if its elliptical orientation was −25 to 155 degrees from vertical in the xy plane with permeability measured along the x-direction). The total porosity of cortical bone was calculated as the total pore volume divided by the total cortical bone volume, the axial porosity was calculated as the axial porous volume divided by total cortical bone volume, and the radial porosity was calculated as the radial porous volume divided by total cortical bone volume. Segmented pore volumes were then imported into MicroView for anisotropy analysis that utilized a mean intercept length approach in which intersections of a test grid composed of lines separated by 3 pixels were passed through each volume at 200 different angles to generate a fabric ellipsoid whose long axis was aligned in the direction of the most prominent structural orientation. Lastly, Euler's number for both the axial and radial components of the segmented porous content of each sample was calculated and divided by total bone ("filled") volume to determine connectivity density (mm^{-3}).

The permeability of each fresh bone wafer was measured three independent times in an endosteal to periosteal direction (i.e., radially) using a customized device (Fig. 1C). A threaded bone holder device was modified from Standard-Wall (Schedule 40) White PVC Pipe Fitting (1/2" Pipe Size, Female Union). Device construction was completed in the Prototype and Polymer Labs in the Department of Biomedical Engineering at the Cleveland Clinic. Bone wafers were placed into a split silicon mold having a centered 5-mm diameter hole, and the entire device was sealed together with a locking ring to withstand against a leak pressure of 1034 kPa (150 psi). PBS solution was then pumped through a 5-mm area of the bone wafers using a 4 MPa limit pump (Pump-P 500, Pharmacia Biotech), at four steady-state flow rates (v): 10, 20, 30 and 40 mL/hr. A maximum backpressure limit of 689 kPa (100 psi) was used for each specimen test in order to avoid device leakage and prevent system failure. To validate that fluid did not flow around the sides of a specimen, a solid stainless steel plate of similar dimensions to the bone wafers was placed into the device and used to block fluid flow. Up to a backpressure of 689 kPa (100 psi), visual inspection showed no fluid leakage.

Fresh and unprocessed bone wafers did not permit fluid flow up to the backpressure limit. Fluid flow through processed bone specimens was monitored to assure steady state flow rates. For each flow rate the pressure difference (Δp) between the upstream fluid and the downstream fluid (atmosphere) was measured with a pressure gauge (Ashcroft Cat # 25D1005PS 02L 100; 100 psi pressure limit). The thickness (L) of each bone wafer was measured with digital calipers (TRESNA, 111-102B; 0.1 mm accuracy) at three different sites along the bone wafer surface. Permeability (P) was then calculated based on Darcy's Law (equation 1):

$$P = \frac{\mu L v}{A \Delta p} \tag{1}$$

where μ is the viscosity of the PBS solution (1 cp = 0.001 kg/(m·s)) and A is the circular surface area of the bone wafer (5 mm diameter) through which the solution flowed. Device accuracy was verified using 316L porous stainless steel filter discs (nominal pore size of 0.5 μm) obtained from Mott Corporation (Farmington, CT) having a reported air permeability of 1.02×10^{-14} m^2. Using our device, we determined that three repeated measures taken from the same filter disc were within ± 2–3% of each other. In addition, we determined that permeability values for three different filter discs were within ± 3–4% of each other.

After permeability assessments of fresh or unprocessed samples were attempted, bone wafers were treated with 10 ml of a 1:1 (v/v) acetone-methanol (AM) (Sigma) solution at 4° C for three days in pre-weighed glass bottles. As an independent assessment for the removal of hydrophobic molecules, some bone wafers were treated instead with 2% w/v 3-[(3-cholamidopropyl)dimethylammonio]-1-propanesulfonate (CHAPS) in PBS at 4° C for 7 days.

CHAPS was used because it is a non-denaturing zwitterionic detergent that is highly soluble in physiological fluids[23], and should not denature the pericellular matrix as much as AM treatment. The volume ratio of AM or CHAPS solution to sample volume was estimated to be a 30-fold volume excess. After treatment the bone wafers were put into new bottles and washed with 10 mL PBS solution three times for 2 hr each time. Permeability of each AM or CHAPS treated bone wafer was measured three times independently (Supplementary Table I).

Proof that the AM treatments of the bone wafers extracted lipids was sought as follows. The AM solutions in their respective sample bottles were placed under a nitrogen stream to evaporate the organic solvents and obtain dried waxy residues. After evaporation, the sample bottles were weighed again and the dry weight of the residues was obtained by taking the difference between the tare weight of each bottle and the weight after AM evaporation. Dry residues were analyzed for phospholipid, free fatty acid and triacylgycerol contents by gas chromatography-mass spectroscopy performed at the Kansas Lipidomics Research Center (Manhattan, KS). Cholesterol was measured spectrophotometrically as previously published.[20]

After measuring permeability of AM- or CHAPS-treated specimens, each bone wafer was then treated with 5 mL of a 100 U/mL bacterial collagenase (type XI, Sigma C-9407) solution in PBS supplemented with 10 μM 4-(2-aminoethyl) benzenesulfonyl fluoride hydrochloride (AEBSF) (Sigma) overnight at 37° C (Supplementary Table II). AEBSF was added to inhibit any serine protease activities potentially contaminating the collagenase preparations. Following collagenase digestion, all bone wafers were washed with 10 mL PBS solution three times for 1 hr each time. Permeability of each collagenase-treated bone wafer was measured three times independently.

Proof of collagenase activity was sought by measuring the amounts of hydroxyl-proline released from the bone wafers into the collagenase solution. Briefly, a 0.5 mL aliquot from each collagenase digestion reaction was placed into Reacti –Vials (Pierce) and frozen overnight at −20° C. The frozen solutions were vacuum dried in a Speed Vac SC110 Concentrator (Savant) for 2 hrs. The dried residues were resuspended in 0.3 mL 6 N hydrochloric acid (HCl; Constant boiling purity for amino acid analysis, Pierce). These vials were placed into a Reacti-Therm III heating module (Pierce) and heated at 105° C for 16 hrs to quantitatively release free amino acids. After acid hydrolysis, a nitrogen gas stream was used to remove the HCl from each sample at 37° C. Each sample was then rehydrated in 0.5 mL of Milli-Q water (Millipore), and their hydroxyl-proline contents were measured by a spectrophotometric method.[2, 24]

After measuring the permeability of collagenase-treated bone wafers, they were then treated with 5 mL of a 1.2 U/mL Dispase (Sigma) solution overnight at 37° C. Following dispase digestion, all bone wafers were washed with 10 mL PBS solution three times for 1 hr each time. Permeability of each dispase-treated bone wafer was measured three times independently. Proof of dispase activity was sought by measuring the amounts of hydroxyl-proline released from the bone wafers into the dispase solution in a manner similar to that described above for the collagenase solution.

Removal of glycoproteins, proteoglycans and hyaluronan from bone wafers resulting from either collagenase or dispase digestion was monitored by amino sugar (glucosamine and galactosamine) and amino acid compositional analysis. Portions of each digestion solution were submitted to 2 N HCl hydrolysis at 105° C for 4 hrs (amino sugar) or 6 N HCl hydrolysis at 105° C for 16 hrs (amino acid). After each hydrolysis, a nitrogen gas stream was used to dry each sample at 37° C. Each sample was then rehydrated in Milli-Q water. The amount of amino acid and amino sugar was analyzed on a Beckman System Gold HPLC Amino Acid Analyzer

by the Molecular Biology Proteomics Facility at the University of Oklahoma Health Sciences Center. Amino acids and amino sugars were detected by on-line post column reaction with ninhydrin. Derivatized amino acids were quantified by their absorption at 570 nm wavelength, except for glutamic acid and proline, which were detected at 440 nm wavelength. A standard containing calibrated amounts of all amino acids was run daily prior to establishing response factors (peak area/nanomole) for each amino acid for each program. Similarly, glucosamine and galactosamine standards were run prior to samples for which quantification of these amino sugars was desired.

After measuring the permeability of dispase-treated specimens, bone wafers were then treated with 20 mL of a 400 mM EDTA (pH 8) (Sigma) solution at 4° C until all of the mineral content was removed (~2–3 weeks). Confirmation of a complete removal of the mineral content of each specimen was obtained by X-ray imaging using micro-CT at an isotropic voxel resolution of 26 μm. Following EDTA decalcification, all specimens were washed with 10 mL PBS solution three times, 30 min each time. Permeability of each EDTA-treated bone wafer was measured three times independently. The remaining insoluble tissue matrix was hydrolyzed with 6N HCl and the total amount of hydroxyl-proline in the remaining tissue matrix after EDTA treatment was measured by a spectrophotometric method as described above, and served as a measure of total insoluble collagen in each sample.

Analysis of the variance (ANOVA) techniques with post-hoc multiple comparison tests were used for statistical analysis (SigmaStat software v3.5). Treatment data was found to be non-parametric, thus repeated measures ANOVA on Ranks and Tukey post hoc multiple comparison tests were run. Given the non-parametric nature of the data populations, quantitative comparisons are reported as the median value in each treatment group. Differences were considered statistically significant if the corresponding ANOVA P-value was less than 0.05.

Results

The structural properties of cortical bone wafers cut from adult canine tibial diaphyses (1.5-mm nominal thickness) were assessed after removing bone marrow and periosteum soft tissues. Micro-CT imaging (Fig. 2A, 3 μm resolution) showed that several pores on both sides of the cortical bone wafers were interconnected across the wafer thickness both radially and axially (Figs. 2B and 2C, respectively). Our calculations showed that the total porosity of adult canine bone wafers was 2.95 ± 0.91%, the radial porosity was 0.60 ± 0.17%, and axial porosity was 2.36 ± 0.71% (Fig. 2D). Connectivity density calculations revealed a value for radial connectivity of 175 ± 87 mm^{-3} and axial connectivity of 438 ± 204 mm^{-3} (Fig. 2E).

Over the entire range of flow rates tested, and without fluid leakage around the manifold, no fluid flowed through fresh or unprocessed bone wafers (1.5-mm thick) up to a tested backpressure of 689 kPa (100 psi). Thus, hydraulic permeability assessments of both fresh and unprocessed cortical bone wafers of 1.5-mm thickness were at or below the detection limit of our system (4.0×10^{-17} m^2). This detection limit is close to the radial hydraulic permeability value previously published for canine tibia by Li et al.[16], 5.0×10^{-17} m^2, and represents an upper limit value for fresh or unprocessed cortical bone.

Cortical bone wafers were submitted to radial hydraulic permeability assessments after sequential treatments to remove lipids (acetone-methanol, AM), digest fibrillar collagen (collagenase), and remove mineral salts (EDTA). All hydraulic permeability assessments after such treatments yielded non-parametric profiles suggesting a high level of heterogeneity and anisotropy in this population of bone wafers (Fig. 3). It should be noted that all bone wafers

showed increased permeability values after subsequent collagenase digestion and EDTA treatment, though individually they exhibited different extents of elevation.

After AM treatment (or CHAPS treatment; Supplementary Table I), the 1.5-mm bone wafers yielded a median permeability value of 8.6×10^{-16} m^2 (Fig. 4). Further the lipids removed from these cortical bone wafers were identified as free fatty acids, phospholipids, triacylglycerols and cholesterol (Fig. 5). In total, these four types of lipids comprised ~76% of the residue's dry weight and accounted for ~9 mg/g wet weight of cortical bone. Triacylglycerols comprised the largest class of lipids (60%), followed by cholesterol (11%), free fatty acids (4%) and phospholipids (1%). The differences in the median permeability values of the unprocessed wafers, which was set at the upper detection limit value of 4×10^{-17} m^2, and bone wafers post AM treatment were found to be statistically different indicating that the removal of lipids elevated cortical bone permeability by at least 21-fold.

After AM treatment, cortical bone wafers were then digested with high purity bacterial collagenase. Permeability of these digested specimens increased to a median value of 1.4×10^{-14} m^2, which is a 16-fold enhancement over that from AM treatment (Fig. 4). To confirm digestion of collagen from these bone wafers, the amounts of hydroxyl-proline released into the collagenase digestion solution (Fig 6, CS) were found to be 63 ± 37 μg hydroxyl-proline/g wet bone. The presence of amino acids in sample digests was used as a measure of released total protein, while the presence of amino sugars was used as a measure of released complex carbohydrates (i.e., glycoproteins, proteoglycans and hyaluronan). Collagenase digestion released relatively small amounts of amino acids (4.2 μmol per g wet bone, Table 1) and amino sugars (0.3 μmol per g wet bone, Table 2). The amino acid composition of the collagenase digested material appeared to be similar to that of the type I collagen standard used in these analyses (Table 1). Altogether these analytical data suggest that the collagenase digestion conditions used in this study released a relatively small amount of collagen-like material from the pericellular matrix in the porous compartment of cortical bone. Overall the differences in the median permeability values of the unprocessed and AM treated bone wafers were found to be statistically lower than those after collagenase digestion indicating that the presence of a collagen matrix within the porous compartment of cortical bone also restricts its permeability.

Subsequent treatment of bone wafers after collagenase digestion with a non-specific serine protease (Dispase, Gibco) did not significantly elevate radial hydraulic permeability values beyond those for collagenase digestion (a median value of 1.6×10^{-14} m^2). Dispase digestion did release an additional 90 ± 110 μg hydroxyl-proline/g wet bone (Fig. 6, DS), 8.8 μmol per g wet bone of amino acids (Table 1), and 1.6 μmol per g wet bone of amino sugars (Table 2). The amino acid composition of the dispase digested material was completely different from that of the type I collagen standard used in these analyses (Table 1) suggesting the release of a more complex array of glycoproteins than that released by collagenase. Altogether, these data indicate that a subsequent digestion with dispase released more hydroxyl-proline, more total amino acids and amino sugars than a prior digestion with collagenase, while not further elevating hydraulic permeability.

All of the above mentioned treatments would have access to the cells and pericellular matrix incorporated only within the porous compartment of cortical bone. The non-porous compartment of cortical bone can only be accessed by removing its calcium mineral salts. After EDTA decalcification, the permeability of the bone wafers was increased to a median value of 6.5×10^{-14} m^2, which is a 5-fold elevation over that from collagenase treatment (Fig. 4). Decalcified bone wafers contained 3100 ± 1800 μg hydroxyl-proline /g wet bone (Fig. 6, bone), 1.1×10^6 μmol per g wet bone of amino acids (Table 1), and 2.0×10^6 μmol per g wet bone of amino sugars (Table 2). The amino acid composition of this insoluble bone matrix material was identical to that of the type I collagen standard used in these analyses (Table 1). Using the

values of hydroxyl-proline recovered from the collagenase and dispase treatments (i.e., porous compartment) and EDTA treatment (i.e., non-porous compartment), the relative proportion of the porous to non-porous collagen content calculates to be 4.9% (= [63 + 90]/3100 × 100%). This relative proportion of hydroxyl-proline contents is close to the average porosity value (~3%) calculated in Figure 2.

Discussion

Removing hydrophobic molecules such as lipids from the porous compartment of cortical bone increased its radial hydraulic permeability. This indicates that the presence of hydrophobic molecules in the porous compartment of cortical bone reduces its permeability and suggests that their presence is a factor influencing fluid flow in cortical bone. In addition, collagenase removal and/or loosening of the collagen pericellular matrix within the porous compartment of cortical bone increased its permeability. This indicates that the orientation and/or packing density of the collagen matrix in the porous compartment of cortical bone restricts fluid flow and represents another factor that influences its overall permeability.

A majority of the extracted hydrophobic content from bone was accounted for by triacylglycerols (60%), cholesterol (11%), free fatty acids (4%) and phospholipids (1%). These findings are consistent with previous studies reporting high levels of triacylglycerols and low levels of phospholipids, within the lipid contents of human[9] or ox[15] cortical bone. This chemical composition suggests that osteocyte cell membranes and any vesicles that bleb off from these membranes are not likely to be a major source of lipids located in the porous compartment of bone since both have a high content of phospholipids.[25, 30] Instead, triacylglycerols comprise the major source of lipids in this bone compartment, and raises an intriguing hypothesis for the source of this hydrophobic material. Triacylglycerols are produced inside most vertebrate cells, including those in the osteogenic lineage, and stored within lipid droplets.[11 25, 30] Takahashi et al.[25] have also shown that osteogenic cells can secrete lipid droplets into their extracellular matrix. Thus, the source of these triacylglycerols extracted from fresh cortical bone might originate from its resident bone cell populations: osteoblasts lining Haversian and Volkmann's canals and osteocytes embedded within the lacuna-canalicular system.

Bone-derived triacylglycerols contain two oleate and one palmitate fatty acyl chains[9] and would present as thick oils or pastes at body temperature. Within the lacuna-canalicular system, this characteristic may imply that these lipids can act as a viscous lubricant to insulate the cell bodies (in lacunae) and fillipodial extensions (in canaliculi) from the mineral crystalline walls. Prior studies have shown that some of these bone-derived lipids exist within the pericellular matrix of osteoblasts and osteocytes[11, 25] and our preliminary microscopy results from Nile Red staining of lipids in cortical bone sections are consistent with this prior knowledge (unpublished data). Given their hydrophobic properties, the presence of lipids in the pericellular matrix of the porous compartment of cortical bone should impede water penetration and contribute to a restriction in its hydraulic permeability.

Densely packed collagen fibers exist in the pericellular matrix of Haversian and Volkmann's canals[4, 7] and surround osteocytes in their lacunae.[7, 28] The orientation, packing density and extent of cross-linking of collagen matrices isolated from bone has been reported to fully exclude the diffusion of molecules ≥ 40 kDa size and partially restrict the diffusion of molecules of 10–15 kDa size.[26] While water can freely diffuse into this collagen matrix, the high concentration of oriented collagen fibers presents a back pressure barrier that slows the rate of fluid movement in this matrix. Thus, densely packed collagen fibers, together with the presence of lipids, form a pericellular matrix that acts as a hydraulic barrier to further compartmentalize fluid flow in the smaller sized lacuna-canalicular system from the larger sized Havesian and

Volkmann's canals. In effect, this hydraulic compartmentalization of the lacuna-canalicular system should emphasize Haversian and Volkmann's canals as the primary conduits of fluid movement in bone ensuring a more efficient transport of hydrophilic nutrients and survival factors over large distances in long bones.

Conventional cell biology axioms dictate that nutrient and metabolic waste product exchange rates are crucial for cell viability and functionality. Yet our findings suggest that such transport phenomena at the lacuna-canalicular level may be severely challenged by low radial hydraulic permeability. Such restrictions certainly emphasize the critical need for mechanical loading as a convection transport mechanism to promote an exchange of nutrients and waste products in cortical bone tissue.[8, 12, 14, 27] Interestingly, the presence of lipids within the pericellular matrix of the lacuna-canalicular system may provide another possible transport process. Lipid-derived, small molecular weight molecules such as prostaglandins, steroids and 1,25-dihydroxy-vitamin D3 can distribute into both hydrophilic and hydrophobic media as a result of their amphipathic chemistry. Perhaps these potent osteogenic molecules can be transported radially within the porous compartment of cortical bone via convection of both aqueous and lipid phases induced by mechanical loading of bone.

Altogether, our findings and the above mentioned discussion leads to the following hypothetical model of transport in cortical bone. In the absence of mechanical loading, small amphipathic molecules would preferentially transport through the lacuna-canalicular system and get to individual osteocytes in a radial direction because of the hydrophobic chemistry of its pericellular matrix and its extremely low hydrophilic fluid permeability. In effect, this may limit the delivery of small molecular weight hydrophilic molecules such as glucose and oxygen to osteocytes, but still allow for some diffusion of prostaglandins, steroids, or 1,25-dihydroxy-vitamin D3 to these same osteocytes. Simultaneously, in the absence of loading, the hydrophobic chemistry and densely packed collagen matrix within the lacuna-canalicular system should restrict access of larger, hydrophilic molecules to movements mostly within the Haversian and Volkmann's canals. In the presence of mechanical loading, hydrophilic fluid (and constituent molecules) would now be pushed through the lacuna-canalicular system, as well as pushed faster through the Haversian-Volkmann's network, via convection forces. These convection forces would increase the transport rate of hydrophilic molecules (glucose) along with hydrophobic molecules (protaglandins) to osteocytes within the lacuna-canalicular system.

Ultimately, if this hypothetical transport model is valid, then the concentration gradients of even small molecular weight molecules within the lacuna-canalicular system will differ based on their hydrophobic/hydrophilic chemistries. Such differences in concentration gradients of small molecular weight molecules in the absence of mechanical loading may impact on bone health. Further investigation of the hydraulic permeability of cortical bone from healthy and diseased bone may help to elucidate its importance to osteophysiology.

Supplementary Material

Refer to Web version on PubMed Central for supplementary material.

Acknowledgments

Funding for this project was provided in part by the Doctoral Dissertation Defense Program of Cleveland State University. We would like to acknowledge the Cleveland Clinic Musculoskeletal Core Center funded in part by a grant from the National Institute of Arthritis and Musculoskeletal and Skin Diseases, No. 1 P30 AR-050953 for microscopic imaging services; the Kansas Lipidomics Research Center for lipid analyses (supported by NSF grants MCB 0455318 and DBI 0521587, NSF EPSCoR grant EPS-0236913 with matching support from the State of Kansas through Kansas Technology Enterprise Corporation and Kansas State University, and NIH Grant P20 RR16475 from the INBRE program of the National Center for Research Resources); and the Molecular Biology Proteomics Facility

at the University of Oklahoma Health Sciences Center for amino acid and amino sugar analyses. We are also grateful to Dr. Matt R. Allen, Assistant Professor in the Department of Anatomy & Cell Biology at the Indiana University School of Medicine, for providing high resolution (3-micron) micro-computed tomography images of our bone wafers.

References

1. Beno T, Yoon Y, Cowin SC, Fritton SP. Estimation of Bone Permeability Using accurate microstructural measurements. J. Biomechanics 2006;39:2378–2387.
2. Berg RA. Determination of 3- and 4- hydroxyproline. Methods in Enzymology. Part A 1982;82:372–398.
3. Berthiaume F, Frangos JA. Fluid flow increases membrane permeability to merocyanine 540 in human endothelial cells. Biochim Biophys Acta 1994;1191:209–218. [PubMed: 8155677]
4. Black J, Mattson R, Korostoff E. Haversian osteons: size distribution, internal structure, and orientation. J. Biomed. Mater. Res 1974;8:299–319. [PubMed: 4426907]
5. Buechner PM, Lakes RS, Swan C, Brand RA. A broadband visoelastic spectroscopic study of bovine bone: implications for fluid flow. Ann Biomed Eng 2001;29:719–728. [PubMed: 11556728]
6. Burger EH, Klein-Nulend J. Mechanotransduction in bone-role of lacunocanalicular network. FASEB J 1999;13:S101–S112. [PubMed: 10352151]
7. Cooper RR, Milgram JW, Robinson RA. Morhpology of the osteon: an electron microscopic study. J Bone Joint Surg Am 1966;48:1239–1271. [PubMed: 5921783]
8. Dillaman RM. Movement of ferritin in the 2- day- old chick femur. Anat. Rec 1984;209:445–545. [PubMed: 6476415]
9. Dirksen TR, Marinetti GV. Lipids of bovine Enamel and dentin and human bone. Calc. Tiss. Res 1970;6:1–10.
10. Hillsley MV, Frangos JA. Review: bone tissue engineering: the role of interstitial fluid flow. Biotechnology and Bioengineering 1994;43:573–581. [PubMed: 11540959]
11. Irving JT, Wuthier RE. Histochemistry and biochemistry of calcification with special reference to the role of lipids. Clin Orthop Rel Res 1968;56:237–260.
12. Johnson MW. Behavior of fluid in stressed bone and cellular stimulation. Calcif Tissue Int 1984;36:S72–S76. [PubMed: 6430527]
13. Klein-Nulend J, van der Plas A, Semeins CM, Ajubi NE, Frangos JA, Nijweide PJ, Burger EH. Sensivity of osteocytes to biomechanical stress in vitro. FASEB J 1995;9(5):441–445. [PubMed: 7896017]
14. Knothe Tate ML, Steck R, Forwood MR, Niederer P. In vivo demonstration of load-induced fluid flow in the rat tibia and its potential implications for processes associated with functional adaptation. J Exp Biol 2000;203(Pt 18):2737–4525. [PubMed: 10952874]
15. Leach AA. The lipids of ox compact bone. Biochem J 1958;69(3):429–432. [PubMed: 13560386]
16. Li GP, Bronk JT, An KN, Kelly PJ. Permeability of cortical bone of canine tibia. Microvasc Res 1987;34:302–310. [PubMed: 2448591]
17. Calden RW, McGeough JA, Barker MB, Court-Brown CM. Age-related changes in tensile properties of cortical bone. The relative importance of changes in porosity, mineralization and microstructure. J. Bone Joint Surg. Am 1993;75(8):1193–1205. [PubMed: 8354678]
18. Muellar KH, Trias A, Ray RD. Bone density and composition: Age-related and pathological changes in water and mineral content. J. Bone and Joint Surg 1966;48-A:140–148.
19. Pietrazk WS, Woodell-May J. The composition of human cortical allograft bone derived from FDA/AATB-screened donor. J. Craniofac. Surg 2005 Jul;16(4):579–585. [PubMed: 16077301]
20. Robinson LG, Pugh ER. The determination of serum cholesterol. US Armed Forces Medical Journal 1957;9(4):501–507.
21. Sander EA, Nauman EA. Permeability of Musculoskeletal Tissues and Scaffolding Materials: Experimental Results and Theoretical Predictions. Critical Reviews in Biomedical Engineering 2003;31(1):1–26. [PubMed: 14964350]
22. Shimko DA, Nauman EA. Development and characterization of a porous poly (methacrylate) scaffold with controllable modulus and permeability. Journal of Biomedical material Research. Part B. Applied Biomaterial 2007;80B:360–369.

23. Simonds WF, Koski G, Streaty RA, Hjelmeland LM, Klee WA. Solubilization of active opiate receptors. Proc Natl Acad Sci USA 1980;77(8):4623–4627. [PubMed: 6254034]
24. Stegemann H, Stalder K. Determination of hydroxyproline. Clinica Chimica Acta 1967;18:267–273.
25. Takahashi T, Ueda S, Takahashi K, Scow RO. pH-dependent multilamellar structures in fetal mouse bone: possible involvement of fatty acids in bone mineralization. American Journal Physiology 1995;266(cell physiology 35):C590–C600.
26. Toroian D, Lim J, Price PA. The size exclusion characteristics of type I collagen-implications for the role of noncollagenous bone constituents. J Biol. Chem 2007;282(31):22437–22447. [PubMed: 17562713]
27. Wang L, Ciani C, Doty SB, Fritton SP. Delineating bone's interstitial fluid pathway in vivo. Bone 2004;34:499–509. [PubMed: 15003797]
28. Weinger JM, Holtrop ME. An ultrastructural study of bone cells: the occurrence of microtubules, microfilaments and tight junctions. Callc. Tiss. Res 1974;14:15–29.
29. Winet H. A bone fluid flow hypothesis for muscle pump-driven capillary filtration: II proposed role for exercise in erodible scaffold implant incorporation. European Cells and Materials 2003;6:1–11. [PubMed: 14562269]
30. Wuthier RE. Lipids of matrix vesicles. Fed. Proc 1976;35(2):117–121. [PubMed: 765160]
31. Zaffe D. Some considerations on biomaterials and bone. Micron 2005;36(7–8):583–592. [PubMed: 16169740]

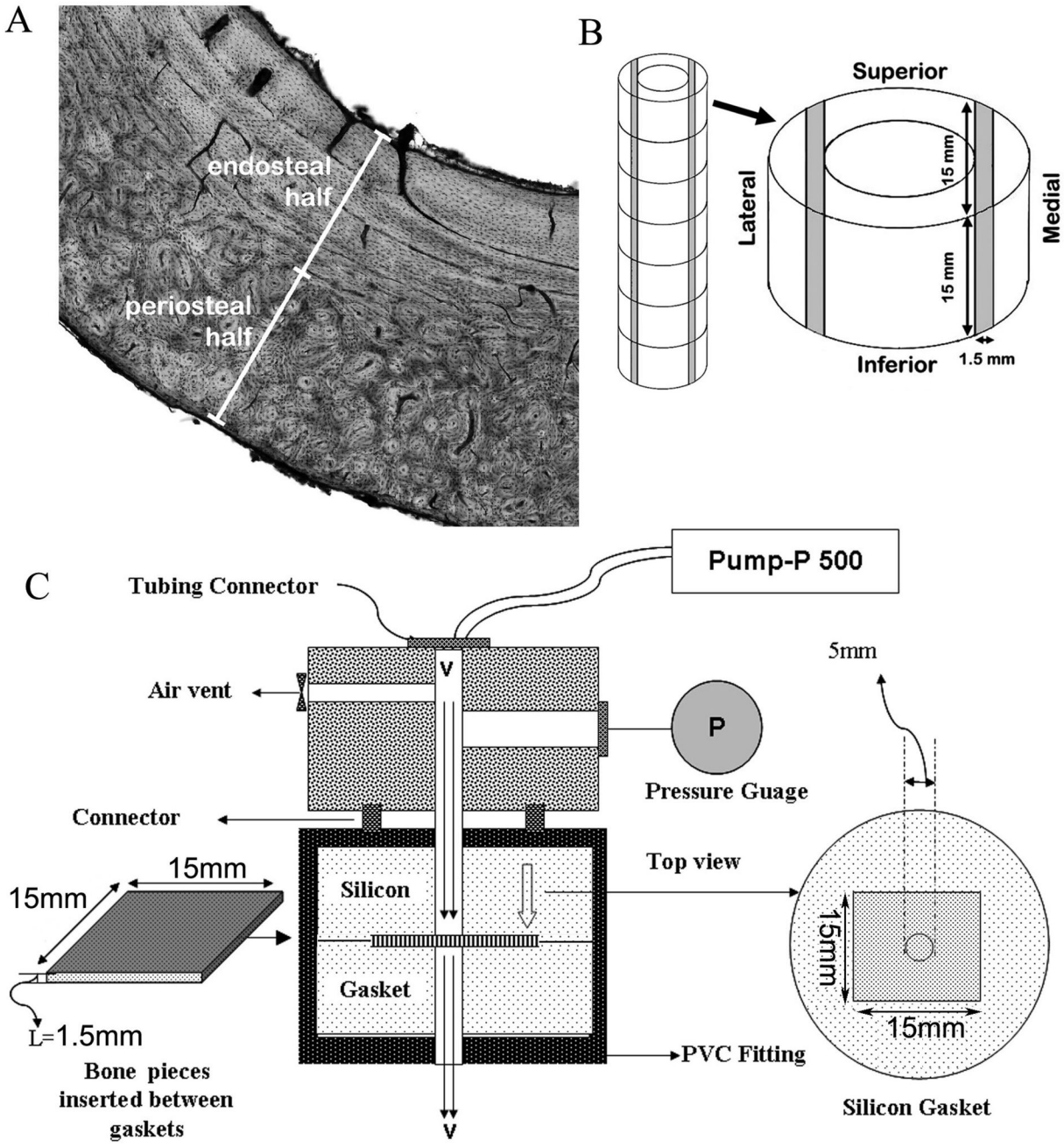

Figure 1. Selection of bone tissue regions and the means to measure hydraulic permeability of cortical bone

Panel A shows a representative histology image of a cross section of canine tibial diaphysis. Panel B illustrates the sampling of cortical bone specimens along the tibial diaphysis length. Shaded areas represent the bone tissue areas from which 1.5-mm thick wafers were produced and analyzed. Panel C shows a schematic of the permeability measurement system.

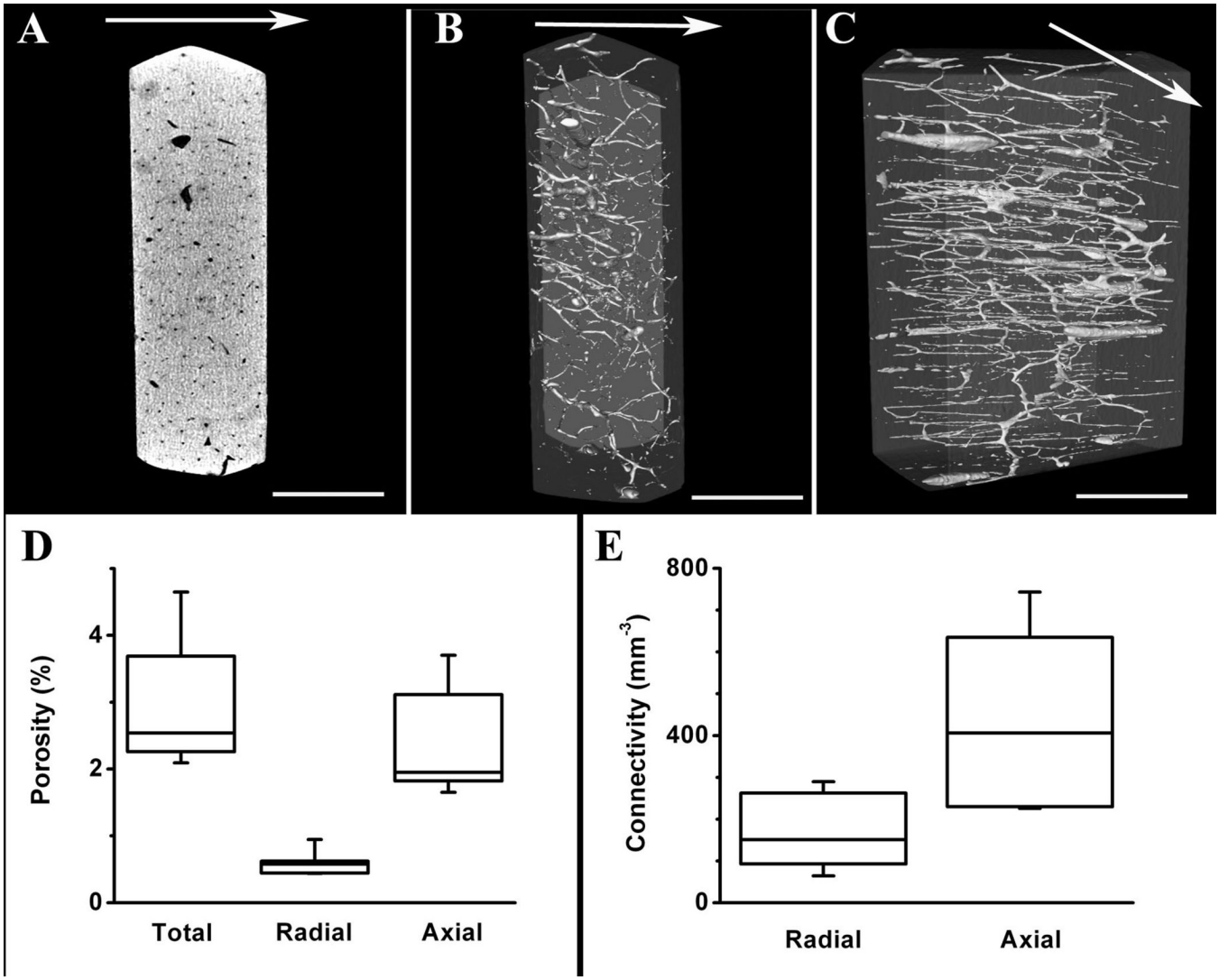

Figure 2. Porosity and connectivity measurements of cortical bone wafers

Panel A shows a representative axial slice of 3D micro-CT bone volume. Panel B shows a representative 3D isosurface rendering of the segmented bone (gray) and segmented pores (white), oriented to visualize radial distribution of pores. Panel C shows the same bone volume as in B, but oriented to indicate the axial distribution of pores (scale bar = 1 mm in all images). *Arrows* in panels A–C show the direction of fluid flow during testing. Panel D shows the total, radial and axial porosity of cortical bone. Panel E shows the radial and axial connectivity of cortical bone. Shown are box and whisker plots exhibiting median (line within the box) and percentiles of the data. The ends of the boxes define 25th and 75th percentiles, and the two whisker error bars define 5th and 95th percentiles.

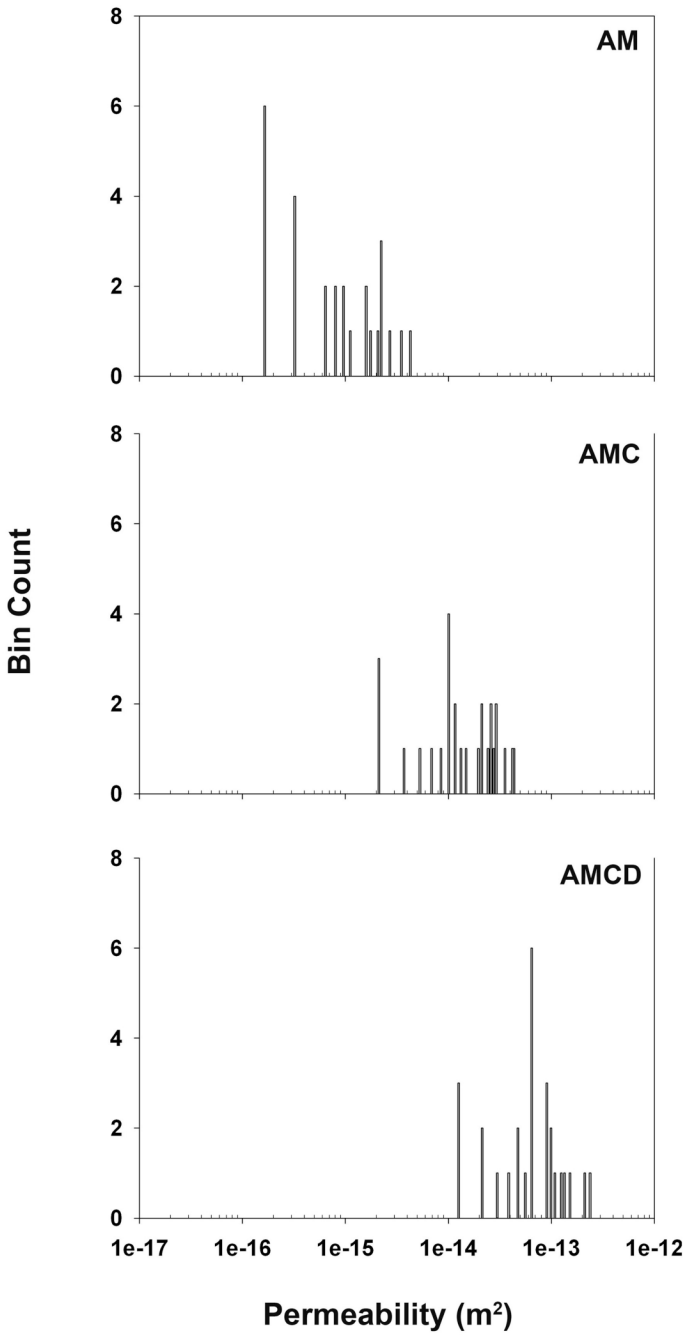

Figure 3. Radial hydraulic permeability measurements of cortical bone wafers after sequential treatments with acetone-methanol, bacterial collagenase, and EDTA

A total of 27 bone wafers were analyzed for radial hydraulic permeability using 3 independent measurements for each processing step. Raw data are presented in a histogram format (27 bins) and depict the non-parametric nature of the radial hydraulic permeability values for this population of bone wafers.

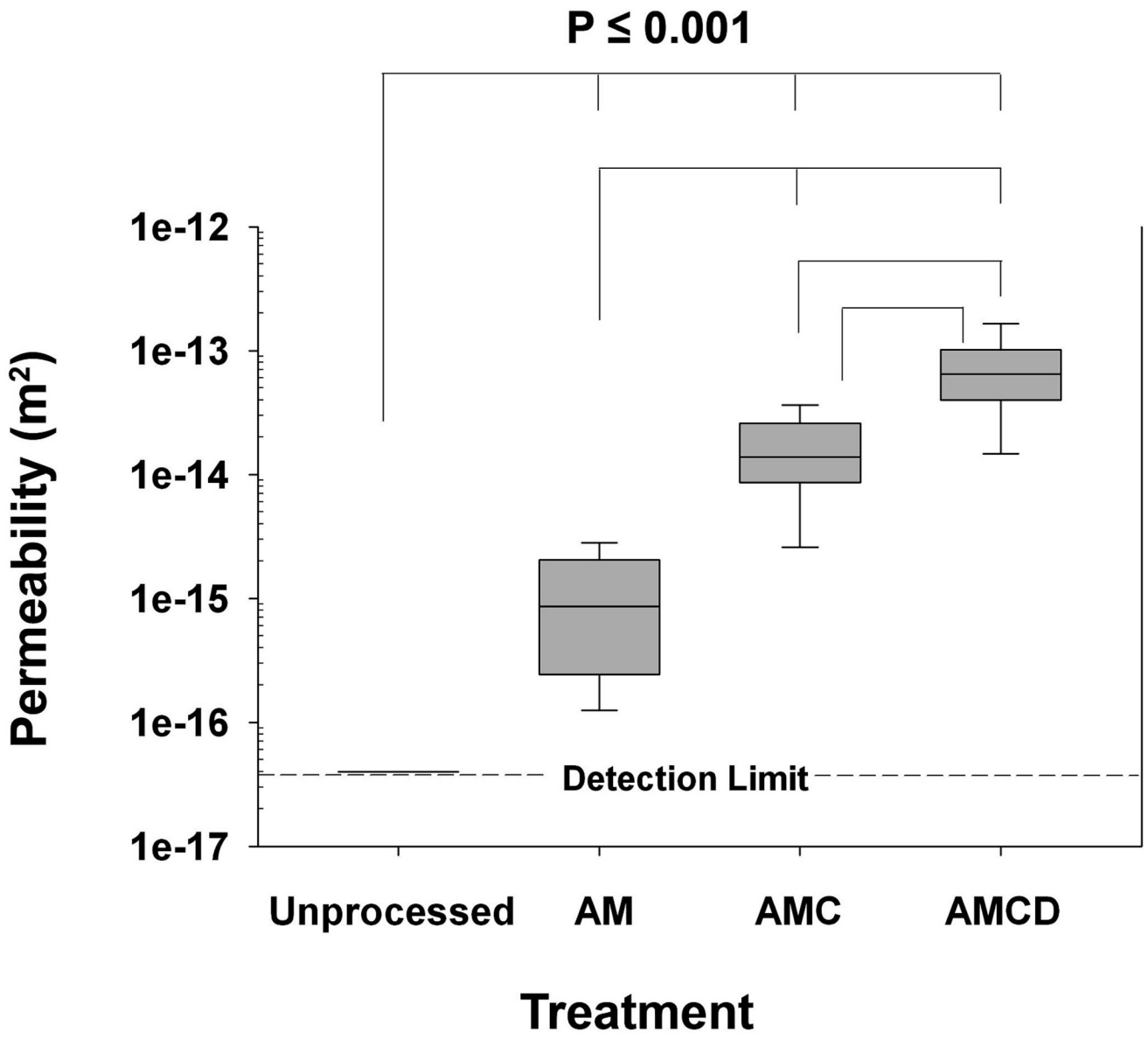

Figure 4. Combined permeability data within each test group

Data are presented in a box and whisker format where whisker error bars represent the 95th and 5th percentiles, the length of each box represents the 75th and 25th percentiles, and the line within the box boundary represents the median value. AM denotes samples treated with acetone-methanol, AMC denotes samples treated with acetone-methanol followed by collagenase digestion, and AMCD denotes samples treated with acetone-methanol then digested with collagenase, and finally decalcified with EDTA. Multiple comparisons of the differences in the median values among the treatment groups were all found to be statistically different from each other ($P < 0.05$).

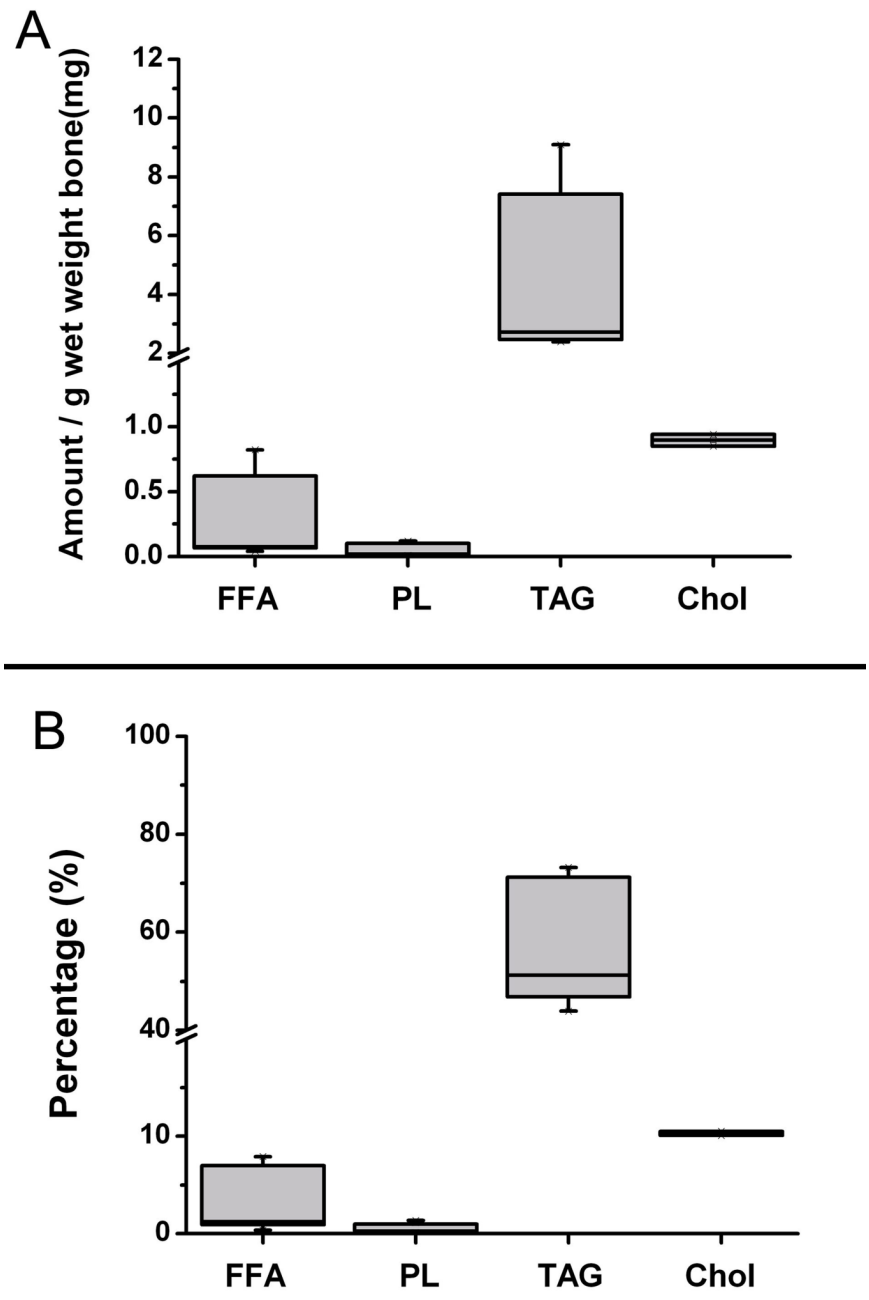

Figure 5. Lipids extracted from cortical bone wafers by acetone-methanol (AM) treatment

Panel A shows the absolute amount of lipids recovered from the AM solutions normalized to the wet weight of each bone wafer. Panel B shows the percentage composition of extracted lipids recovered from the AM solutions. *FFA*: Free fatty acids; *PL*: Polar lipids; *TAG*: Triacylglycerols; and *Chol*: Cholesterol.

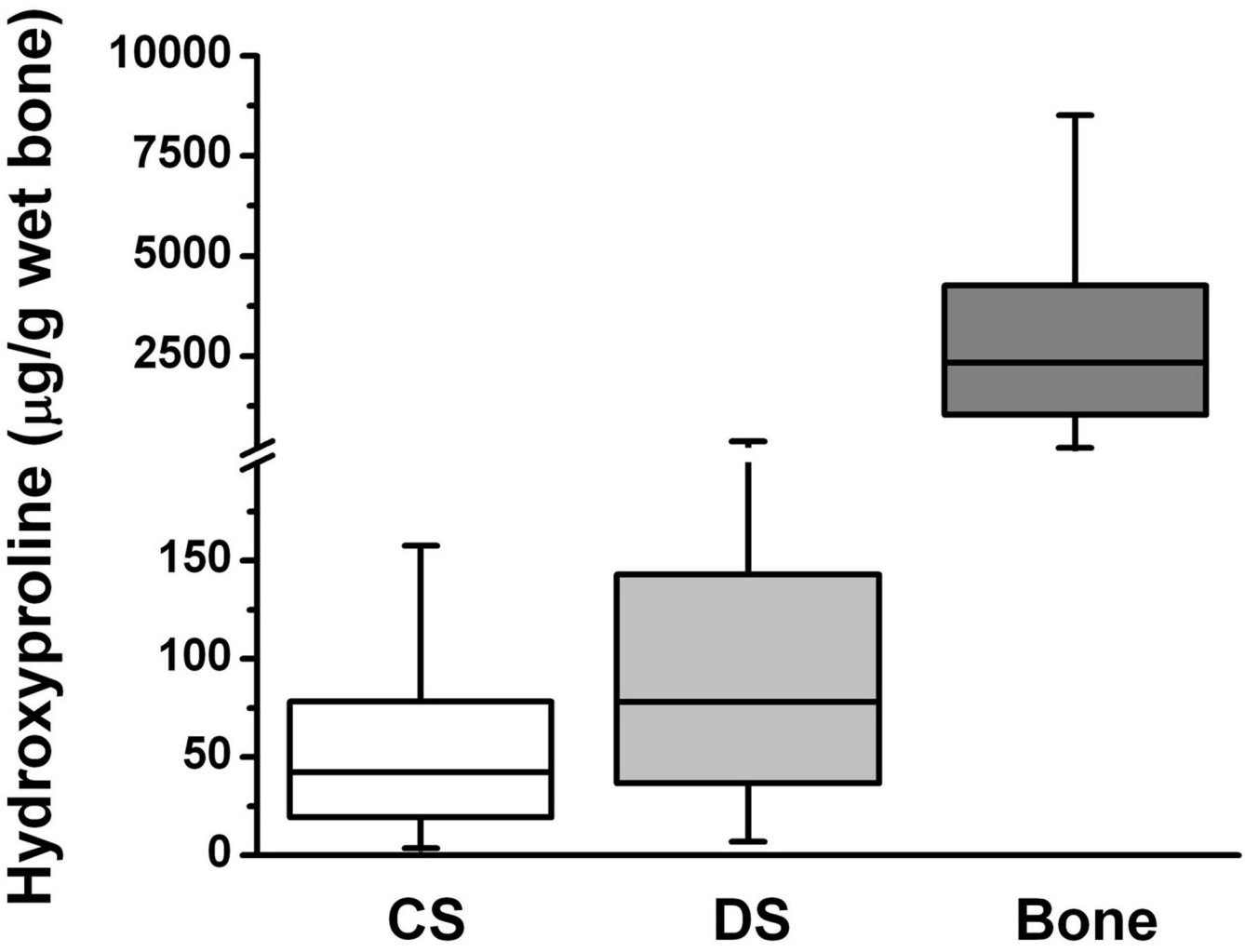

Figure 6. Amounts of hydroxyl-proline released from cortical bone wafers by collagenase or dispase digestions

CS represents the amount of hydroxyl-proline released into solution from the porous compartment of bone wafers by bacterial collagenase digestion. *DS* represents the amount of hydroxyl-proline released into solution from the porous compartment of bone wafers by dispase digestion. *Bone*, represents the amount of hydroxyl-proline in the insoluble collagenous matrix within the non-porous compartment after complete decalcification of bone wafers using EDTA.

Table 1

Amino acid (AA) analyses performed on digest solutions collected from collagenase- and dispase-treated bone wafers.

Amino acid [1]	Collagenase released (CS) [2] µmol (mol %)	Dispase released (DS) [3] µmol (mol %)	Insoluble bone organic matrix (Bone) µmol × 10^6 (mol %)	Type I collagen Standard µmol × 10^3 (mol %)
Asp+Asn	1.9 (6%)	11.3 (16%)	0.5 (6%)	1.0 (5%)
Thr	0.8 (2%)	4.1 (6%)	0.2 (2%)	0.4 (2%)
Ser	1.4 (4%)	9.7 (14%)	0.3 4%)	0.9 (5%)
Glu+Gln	4.1 (12%)	28.8 (41%)	0.7 (8%)	1.5 (8%)
Pro	6.5 (19%)	5.0 (7%)	1.2 (14%)	2.5(14%)
Gly	9.0 (27%)	7.9 (11%)	3.4 (38%)	6.9 (37%)
Ala	4.4 (13%)	nd	1.2 (13%)	2.4 (13%)
Cys	nd	nd	nd	nd
Val	1.1 (3%)	nd	0.1 (1%)	0.3 (1%)
Met	0.1 (<1%)	nd	0.1 (<1%)	0.1 (<1%)
Ile	0.3 (1%)	0.5 (1%)	0.1 (<1%)	0.1 (<1%)
Leu	2.1 (6%)	nd	0.3 (3%)	0.6 (3%)
Tyr	nd	nd	0.04 (<1%)	0.1 (<1%)
Phe	0.1 (<1%)	nd	0.1 (2%)	0.3 (1%)
Lys	0.2 (<1%)	2.6 (4%)	0.3 (3%)	0.6 (3%)
His	0.7 (2%)	1.2 (2%)	0.02 (<1%)	0.1 (<1%)
Arg	2.0 (6%)	2.0 (3%)	0.5 (5%)	1.0 (6%)
AA TOTAL	34.7	73.2	9.1	18.7
Normalized AA TOTAL [4] (µmol/g wet bone weight)	4.2	8.8	1.1×10^6	--
% recovered (CS+DS+Bone)	< 0.1%	< 0.1%	99.9%	--

[1] Digest solutions, EDTA treated bone wafers and type collagen standard were acid hydrolyzed and processed for AA analyses as described in the materials and methods. Results were obtained by combining 3 bone wafers per sample. EDTA treated bone wafers (same bone wafers) and a type 1 collagen standard served as AA collagen content controls. The gray shaded residues represent the major AAs of type 1 collagen.

[2] The baseline AA content contribution from the collagenase enzyme was accounted for and subtracted from analyzed collagenase digest samples.

[3] The baseline AA content contribution from the dispase enzyme was accounted for and subtracted out from analyzed dispase digest samples.

[4] The combined wet weight of the analyzed bone wafers (n = 3) was 8.4 g.

Table 2

Amino sugar (AS) analyses performed on digest solutions collected from collagenase-treated, dispase treated and EDTA treated bone wafers.

Amino sugar [1]	Collagenase released (CS) [2] µmol (mol %)	Dispase released (DS) [3] µmol (mol %)	Insoluble bone organic matrix (Bone) µmol × 10^7 (mol %)
Glucosamine	1.3 (59%)	7.9 (59%)	1.1 (64%)
Galactosamine	0.9 (41%)	5.5 (41%)	0.6 (36%)
TOTAL	2.2	13.4	1.7
Normalized AS TOTAL [4] (µmol/g wet bone weight)	0.3	1.6	2×10^6
% recovered (CS+DS+Bone)	< 0.1%	< 0.1%	99.9%

[1] Digest solutions and EDTA treated bone wafers were acid hydrolyzed and processed for AS analyses as described in the materials and methods. Results were obtained by combining 3 bone wafers per sample.

[2] The baseline AS content contribution from the collagenase enzyme was accounted for and subtracted from the analyzed collagenase digest samples.

[3] The baseline AS content contribution from the dispase enzyme was accounted for and subtracted out from the analyzed dispase digest samples.

[4] The combined wet weight of the analyzed bone wafers (n = 3) was 8.4 g.